Synthesis of Polyaniline Nanostructures in Micellar Solutions

Fawzia. I. El-Dib, Wafaa M. Sayed, Sahar. M. Ahmed, Mohamed Elkodary

Petrochemical Department, Egyptian Petroleum Research Institute, Nasr City, Cairo, Egypt

Received 14 October 2010; accepted 9 July 2011
DOI 10.1002/app.35231
Published online 4 November 2011 in Wiley Online Library (wileyonlinelibrary.com).

ABSTRACT: Polymerization of aniline nanoparticles was carried out in aqueous micellar solutions of surfactants, including anionic (sodium dodecyl sulfate), nonionic (nonyl phenol ethoxylate), and cationic (cetyltrimethyl ammonium bromide) surfactants. The size and morphology of these synthesized PANI nanoparticles strongly depended on the structure of the surfactants used in the formation of micelles, as shown by transmission electron microscopy. Scanning electron microscopy, Fourier transform infrared spectroscopy, and X-ray diffraction were used in the characterization of the synthesized PANI nanoparticles. The PANI nanoparticles revealed enhanced conductivity compared to conventional bulk PANI. In addition PANI–poly(methyl methacrylate) (PMMA) nanocomposites were synthesized. The results revealed that the PMMA nanoparticles retarded thermal decomposition and enhanced the conductivities compared with pristine PANI nanoparticles. © 2011 Wiley Periodicals, Inc. J Appl Polym Sci 124: 3200–3207, 2012

Key words: nanoparticle; polyester; surfactants

INTRODUCTION

Intrinsically conductive polymers (ICPs) are considered an attractive subject of research because of their potential applications in multidisciplinary areas, such as electrical, electronics, thermoelectric, electrochemical, electrorheological, chemical, membrane, and sensor applications.[1–4] Among the available ICPs, polyaniline (PANI) is one of the most promising conducting materials because of its ease of synthesis, low-cost monomer, remarkable environmental stability, tunable properties, and better stability compared to other ICPs. On the basis of these superiorities, PANI has been applied in the fields of antistatic materials, anticorrosion coatings, batteries and energy storage, organic light-emitting diodes, and chemical sensors.[5–9]

A useful approach to overcoming some of the physical and chemical limitations, including the processability and mechanical and thermochemical stabilities of ICPs, involves the combination of these materials with other well-known nonconducting polymers, such as poly(vinyl alcohol), polystyrene, poly(methyl methacrylate) (PMMA), and poly(vinyl acetate).[10] The resulting composites combine the advantageous electrical, redox, or optical properties of ICP with mechanical properties of the host polymer through the ratio of ICP versus the insulting polymer.[11] Consequently, there is a wide scope for the practical applications of such composites.[12–20] PMMA is used to improve the mechanical properties and processability of PANI. PMMA is chosen as a dielectric matrix because of its high transparent ability in the visible spectral range, which is important for optoelectronics, sensors, and smart-window applications.[21]

Recently, several researchers synthesized polymer nanoparticles using microemulsion polymerization.[22–26] This approach uses nanometer-sized micelles as nanoreactors, which are formed from the self-assembly of surfactant molecules in solvent. Therefore, the morphology of the resultant polymer nanoparticles is largely dependent on the micelle structure derived from the surfactant assembly, such as spherical, cylindrical, and layer structures. In this article, we report the fabrication of PANI nanostructures with microemulsion polymerization. The size of the PANI nanoparticle was controlled as a function of different surfactants (anionic, cationic, and nonionic). In addition, we also investigated the conductivity of PANI nanoparticles as dependent on the type of surfactant. This study was also focused on the preparation of nanocomposites with the prepared PANI nanoparticles and methyl methacrylate (MMA). The thermal and electrical properties of the nanostructured PANI/PMMA composites were investigated.

EXPERIMENTAL

Materials

The aniline monomer (99.5%), ammonium peroxydisulfate (APS), sodium dodecyl sulfate (SDS; 99%),

Correspondence to: W. M. Sayed (wafaamahmoudsayed@hotmail.com).

nonyl phenol exthoxylate (NPE), and cetyltrimethyl ammonium bromide (CTAB) were obtained from Aldrich Chemical Co. We also used benzoyl peroxide (Fluka, (Buchs, Switzerland) purum, moistened with water, $\geq$97.0%), MMA (Aldrich, steinheim, Germany), and toluene (Sigma-Aldrich, $\geq$99.9%)

Measurements

Fourier transform infrared (FTIR) spectra

The FTIR spectra of the synthesized PANIs were recorded on a PerkinElmer (France) 1720 FTIR spectrometer.

Thermogravimetric analysis (TGA) measurements

TGA of the synthesized PANIs was carried out on a TA Instruments SDTQ 600 simultaneous (Crawly, United Kindom) TGA–differential scanning calorimetry thermogravimetric analyzer. The samples were heated under a nitrogen flow (100 mL/min) from 50 to 800°C at 20°C/min.

Conductivity measurement

The PANI samples were pressed into pellets in a hydraulic press (model WT-324, Kimaya Engineers, India) at 5 metric tons of pressure. We determined the bulk conductivity of the different polymer samples by pressing them into pellets 1.33 cm in diameter and 1 mm thick. The conductivity measurements were carried out by a four-probe technique recorded by a Keithley electrometer (model 6517A). The pellets used in this measurement were placed between two copper electrodes, which were connected to the two terminals of the Keithley electrometer.

Transmission electron microscopy (TEM)

The microstructures of the synthesized PANIs were examined by TEM (Tokyo, Japan) on a JEOL JEM-2000EX (Tokyo, Japan) at an accelerating voltage of 100 kV.

Scanning electron microscopy (SEM)

The emission SEM (Tokyo, Japan) was performed with a JEOL 5400 (Tokyo, Japan) scanning electron microscope.

X-ray diffraction (XRD)

XRD (Almelo, Netherelands) patterns were recorded on a Pan Analytical model X'Pert Pro (Almelo, Netherelands) with Cu Kα radiation (1.54 Å) at 40 kV and 40 mA in the 2θ range 10–80°.

Synthesis of the PANI nanostructures

A stock micelle solution was prepared by the dissolution of the surfactants into distilled water with continuous stirring. The micelles were formed spontaneously as the concentration of the surfactant in the solution was greater than its critical micellar concentration (cmc).

In a typical fabrication of PANI nanoparticles, 1 g (10.7 mL/mol) of aniline monomer was added dropwise to 40 mL of the surfactant solution (0.5*M*), and 1.23 g (5.3 mL/mol) of APS and 22 g (33 mL/mol) of 1.5*M* HCL were added to the mixed solution. The chemical oxidation polymerization proceeded with magnetic stirring for 3 h at 3°C. After polymerization, the reaction product was placed in a separating funnel. Excess ethanol and distilled water were poured into the funnel alternatively to remove surfactants and to precipitate the PANI nanoparticles. The PANI nanoparticles were retrieved and dried in a vacuum oven at room temperature.[27]

Several PANI nanoparticles were synthesized with different types of surfactants (SDS, NPE, and CTAB) to investigate the morphology, conductivity, and TGA. For comparative purposes, PANI without surfactants was also synthesized under similar conditions.

Preparation of the PANI–PMMA nanocomposites

The PANI–PMMA nanocomposites were synthesized *in situ* to make transparent conducting composites.

A typical procedure for the preparation of PANI–PMMA composites was followed, which involved the placement of 20 mL of MMA, 0.15 g (0.75%) benzoyl peroxide in 20 mL of toluene, and 0.5 g of PANI powder into a 250-mL three-necked, round-bottom flask, and the solution was stirred for 1 h at 80°C to complete the polymerization of the monomer. Nitrogen was bubbled into the flask through the reaction. The product was washed and dried at 100°C for 24 h *in vacuo* to yield the PANI/PMMA composite.

RESULTS AND DISCUSSION

First, a micellar solution was prepared by the dissolution of the surfactant in distilled water with the concentration over its cmc. It has been well established that surfactants will aggregate spontaneously to form micelles when the concentration is over their cmc. Because of the presence of the hydrophobic micellar core and hydrophilic interface, these micelles are capable of dissolving water-insoluble substances.[28] A certain amount of aniline is added to the solution to be loaded onto the micelles. The loading of aniline onto the micelles is a process that is driven

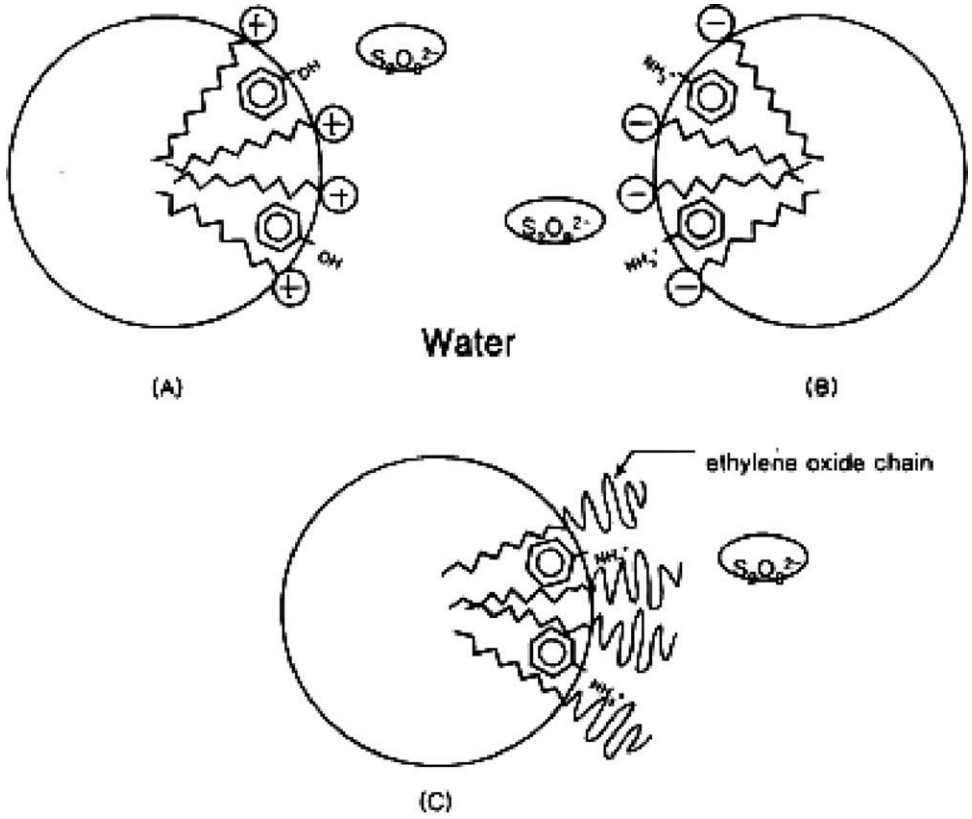

Scheme 1 Schematic diagram for the solubilization locus of aniline–HCl salt in (A) CTAB, (B) SDS, and (C) NPE micelles.

by both the hydrophobic and electrostatic forces. These micelles may serve as templates to orient and organize the aniline molecules in the solution. In this specific system, aniline monomer may have been intercalated between the surfactants as components of the micelles[29] or located in the Stern layer surrounding the surface of micelles. The orientation or organization of aniline molecules in the micelle solutions may have affected the regioselectivity of the reaction.

Different types of surfactants with different molecular structures were selected to form the micelle templates for the polymerization of aniline. The difference in the behavior of the polymerization of aniline in various micelle solutions could be explained by the variation of the local environment formed by different surfactants. In all of these micelle solutions, hydrophobic cores were formed; however, the hydrophilic interfaces of the micelles were quite different because of the differences in the head-group structure of the surfactants. The head group of NPE was polyoxyethylene, with nine repeat units without any charge. Therefore, a neutral hydrophilic interface was formed around the NPE micelles in the solution. The long ethylene oxide chain in NPE effectively hindered the sulfate ions (oxidant, APS) from attacking the anilinium cation in the micelles. Thus, the formation of PANI particles in NPE micelles was very slow because the disulfate ions should have diffused through the films formed by the ethylene oxide chains to initiate polymerization. Therefore, the NPE micelles produced two different sizes of particles. The large particles, which precipitated in the middle of the reaction, were initiated from anilinium ions located outside the NPE micelles, and the small particles were from anilinium ions solubilized in micelles. No electrostatic interactions between the head group of NPE and the charged aniline or other species were expected at the hydrophilic interface of the micelles.[29] On the other hand, if a positively charged hydrophilic region in the CTAB micelle solution was formed, anionic species such as OH— would have been likely attracted in this region through electrostatic interaction. The condensation of OH species in the Stern layer would have led to a higher pH in the local environment of the micelles compared to the bulk solution. When oxidant APS was added to the reaction system, the electrical interaction between anionic disulfate ions and anilinium cation occurred, and the polymerization took place at nanoscale micelles and was then followed by PANI growth. The micelles formed by surfactants such as SDS had negatively charged interfaces in the solution. In strong acidic solution (HCl), the SDS micelles would have had a low micellar surface charge because the ionization degree of the ionic

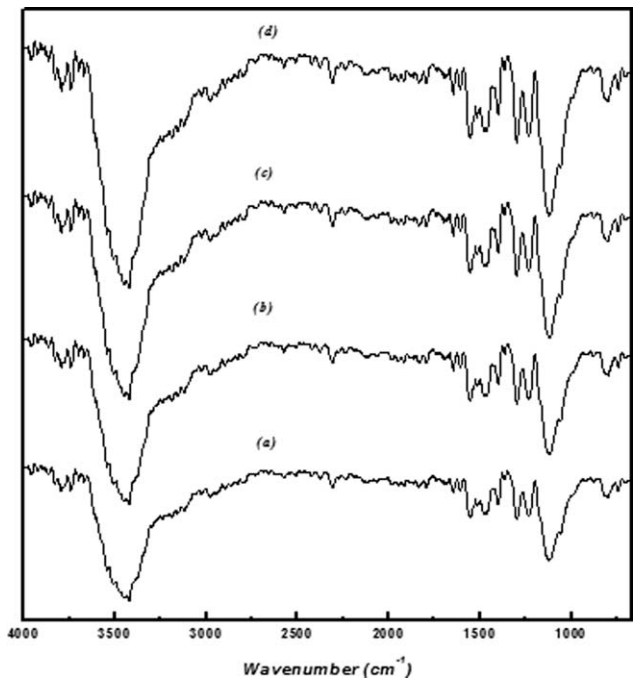

Figure 1 FTIR spectra of PANI synthesized in (a) cationic, (b) anionic, and (c) nonionic surfactants and (d) without surfactants.

surfactant was smaller than that in neutral solution. Furthermore, the cationic anilinium ions would have decreased the anionic net charge of the SDS micelles by solubilization in the micellar surface. Thus, the surface of SDS micelles in the experimental conditions would have had a low net negative charge. This net negative charge of the micellar surface retarded the approach of disulfate ions into anilinium ions; this resulted in a slower reaction rate in the SDS micellar solution compared to that in the bulk aqueous solution. Different types of micellar aggregates may have been formed when the surfactant concentration was above the cmc, and consequently, this may have altered the shape of the nanoparticles of PANI. Micelle-assisted synthesis was previously used widely to prepare polymer particles in which the particle sizes were controlled by the micelle reactor sizes (Scheme 1).[30]

FTIR spectroscopy

Figure 1 presents the FTIR spectra of the prepared PANI nanoparticles. The main characteristic bands of PANI were assigned as follows. The characteristic sharp band at 1220–1020 cm^{-1} was due to C—N tertiary aromatic vibrations. The bands at 1360, 1250, 1340, and 1310 cm^{-1} were due to C—N primary and secondary vibrations. The sharp characteristic band at 3450–3200 cm^{-1} was due to single-bridge compound polymeric association or to NH stretching vibrations. The bands at 1550 and 1475 cm^{-1} were due to the presence of the quinoid structure, and the band at 1240 cm^{-1} was due to the C—N stretching mode for the benzenoid ring. The band at 810 cm^{-1} was attributed to the out-of-plane bending vibrations of C—H on the para-substituted aromatic ring.

Morphology of the PANI nanoparticles

The TME images of PANI nanoparticles synthesized in SDS micellar solution appeared as rod shapes [Fig. 2(a)], and their diameter sizes varied from 34 to 63. Missel et al.[31] reported that the size of particles formed in micelles was closely correlated with that of the micelles.

In our study, we expected that because of the acidic reaction conditions, the ionization of SDS molecules would be depressed and result in a decrease of the electric negative charge. Furthermore, the cationic anilinium ions would decrease the anionic net charge of SDS micelles by solubilizing in the micellar surface. Thus, the surface of the SDS micelles in the experimental conditions would have a low net

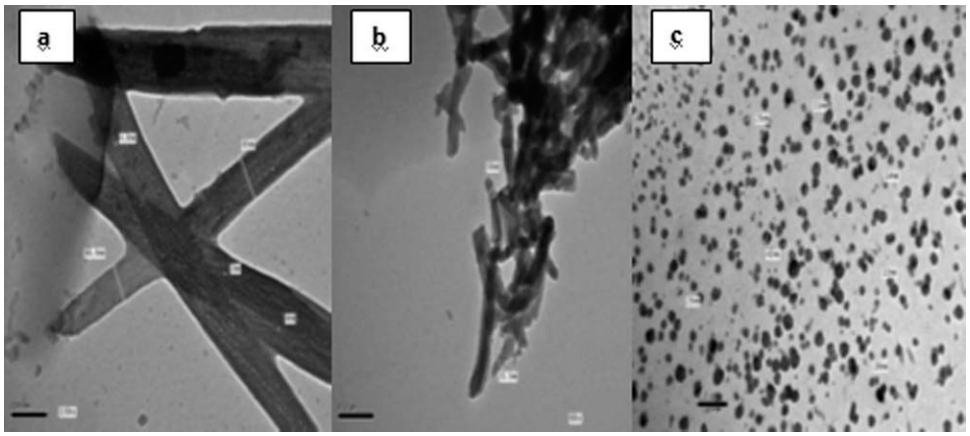

Figure 2 TEM of nanoparticle PANI synthesized in (a) anionic, (b) cationic, and (c) nonionic micellar solutions.

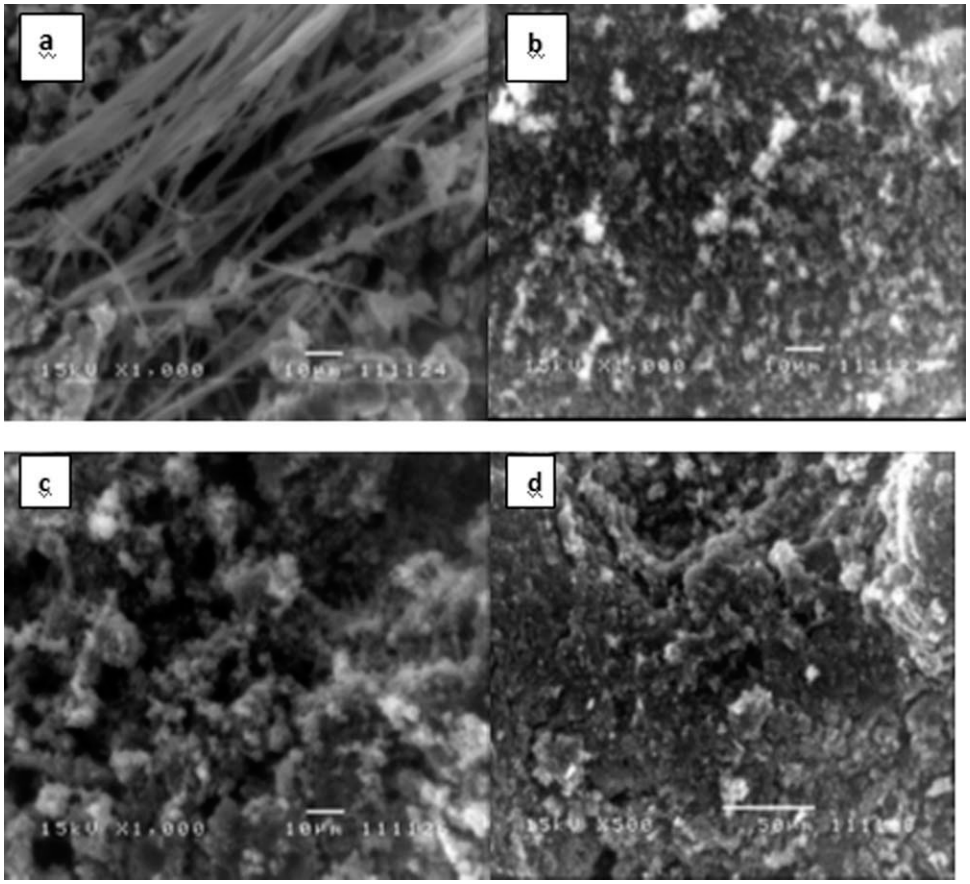

Figure 3 SEM images of PANI synthesized in (a) anionic, (b) cationic, and (c) nonionic surfactants and (d) without surfactants.

negative charge and result in a decrease of the electric repulsion between the surfactant head groups. This reduction in the electrical repulsion and relatively high SDS concentration (>cmc) might have increased the aggregation number and micellar size. In these reaction conditions, the deviation of micellar shape from spherical could not be excluded.[32,33] Figure 2(b) presents the TEM image of the PANI nanoparticles polymerized with CTAB micelles, which appeared as homogeneous rod shapes 43–45 nm in diameter. In the NPE micellar solution, some precipitates, which had a slightly spherical shape and ranged from 14 to 23 nm in diameter, were observed, as shown in the TEM image in Figure 2(c).The large particles formed outside the micelles, and the small particles formed inside the micelles. It was interesting to see that the shapes of these large particles were spherelike and irregular and ranged from 20 to 42 nm in diameter, even though they were formed outside the micelles in solution.

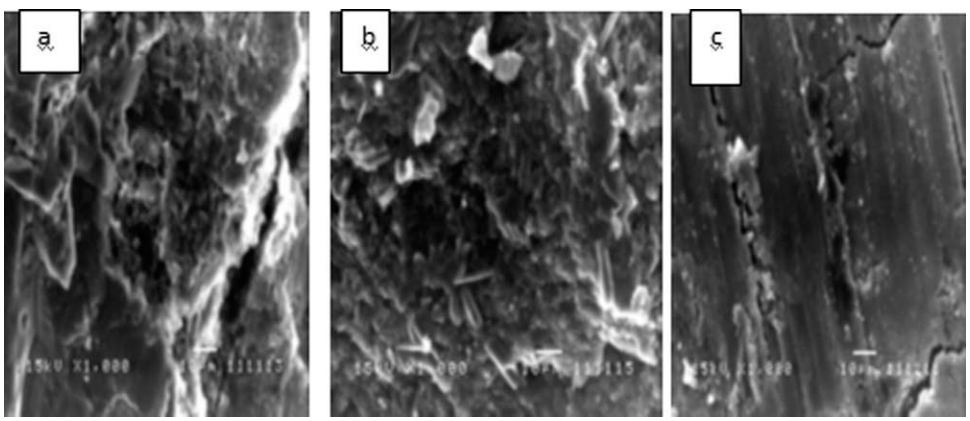

Figure 4 SEM images of PANI–bulk/PMMA, (b) PANI–CTAB/PMMA, and (C) PANI–NPE/PMMA.

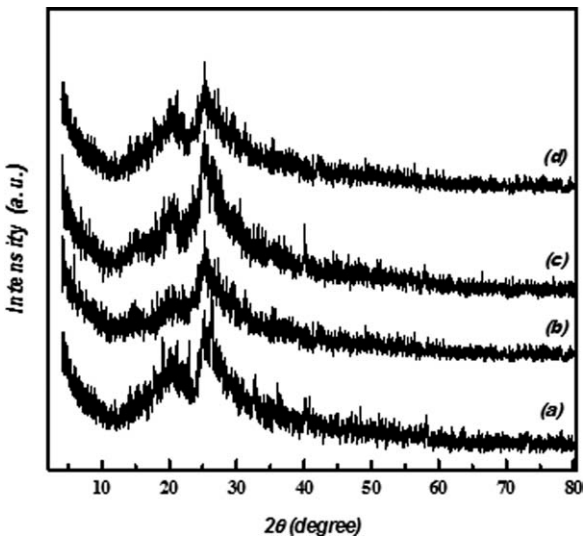

Figure 5 XRD patterns of PANI synthesized in (a) anionic, (b) cationic, and (c) nonionic surfactants and (d) without surfactants.

From the SEM images of the PANI and PANI–PMMA composite prepared *in situ* without surfactants, as shown in Figures 3(d) and 4(a), it was clear that there were irregular forms of PANI incorporated with PMMA. In addition, the SEM photographs of the pristine PANI nanoparticles and PANI–PMMA nanocomposite with CTAB as a micellar template are shown in Figures 3(b) and 4(b). The morphology of the PANI–PMMA nanorods in this micrograph were PMMA nanoparticles surrounded by irregular forms of nano-PANI, whereas the morphology of the original PANI nanoparticles and PANI–PMMA nanocomposite were determined after polymerization with NPE as a micellar template. As shown in Figures 3(c) and 4(c), the spherelike PANI nanoparticles were well dispersed into the PMMA polymer matrix, and no free PANI nanoparticles were observed

XRD

The XRD analysis is presented in Figure 5. The XRD patterns of the PANI nanoparticles synthesized with different types of surfactants (anionic, nonionic, and cationic) exhibited sharp peaks at 2 θ = 20 and 26°; this indicated the presence of a high crystallinity and condensed structure. The peak centered at 2 θ = 20 was ascribed to the periodicity parallel to the polymer chain, and the latter peak may have been caused by the periodicity to the polymer chain.[34] The profiles of the XRD patterns of the PANI nanoparticles were similar to that of PANI, as shown in Figure 5(a–d). These results were consistent with the results of the FTIR analysis. For that, there was no difference between the PANI and PANI nanoparticles.

TABLE I
Conductivity of the Synthesized PANI Nanoparticles and PANI/PMMA Nanocomposites

Sample	Conductivity
PANI–bulk	$0.149761132 \times 10^{-10}$
PANI–CTAB	$0.44338987 \times 10^{-10}$
PANI–NPE	$0.163832413 \times 10^{-9}$
PANI–SDS	$0.112261725 \times 10^{-9}$
PANI–bulk/PMMA	$8.823467379 \times 10^{-10}$
PANI–CTAB/PMMA	$1.777364218 \times 10^{-9}$
PANI–NPE/PMMA	$6.831639054 \times 10^{-9}$

Conductivity

Table I shows that the conductivities of the PANI nanoparticles prepared in SDS, CTAB, and NPE micelles were highest compared with those of the particles formed in bulk aqueous solution according to the following order:

$$\text{NPE} > \text{SDS} > \text{CTAB} > \text{Bulk aqueous solution}$$

This may have been due to the fact that, because the polymerization reaction in surfactant micellar solution occurred in the confined space of micelles, the density of the PANI particles formed was higher than that of particles formed in bulk aqueous solution.[35] PANI nanoparticles can be applied as optically transparent conducting materials because of their high conductivity and ultrafine nanosize.

In general, PMMA is a typical transparent, amorphous polymer and has been used for glass substitutes. PANI nanoparticles synthesized in CTAB and NPE that had average particle diameters of 43–45 and 13–42 nm, respectively, were selected for this experiment. Therefore, PANI–PMMA composites with and without CTAB and NPE micelle templates were synthesized. The conductivity results are shown in Table I. Interestingly, the conductivity of pristine PANI increased continuously after the PANI–CTAB and PANI–PNE nanocomposites were

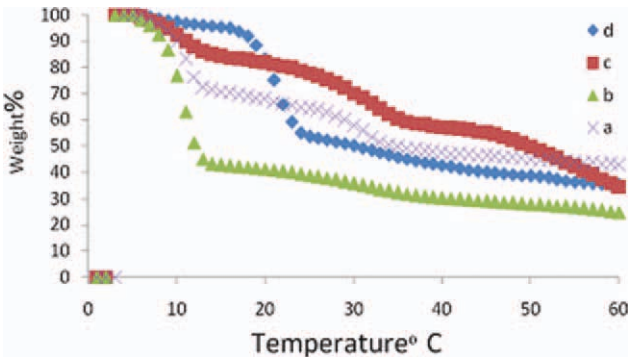

Figure 6 TGA of PANI in (a) anionic, (b) cationic, and (c) nonionic surfactants and (d) without surfactants. [Color figure can be viewed in the online issue, which is available at wileyonlinelibrary.com.]

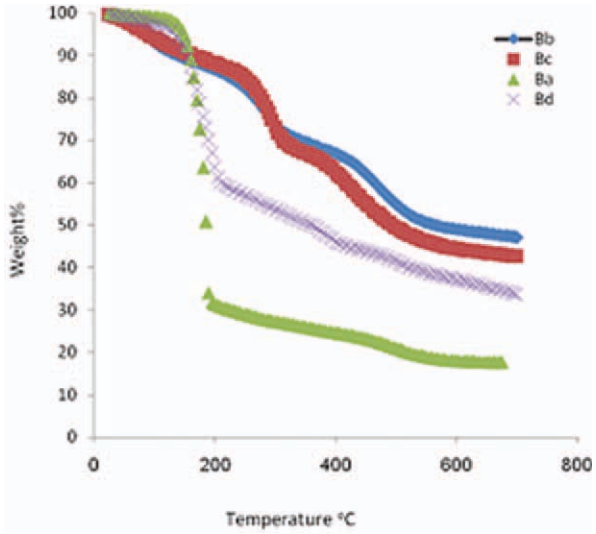

Figure 7 TGA of PANI in (a) anionic, (b) cationic, and (c) nonionic surfactants and (d) without surfactants after blending with PMMA. [Color figure can be viewed in the online issue, which is available at wileyonlinelibrary.com.]

prepared with PMMA. The increases in the electrical conductivity may have been due mainly to the strong interaction of PANI imine nitrogen by the PMMA ester functional group,[35] and also, the formation of electronic paths was favorable with the presence of filler, which was ultrafine PANI nanoparticles.

This interpretation, in agreement with Amrithesh et al.,[36] explained that in the PANI–PMMA composites, the conducting PANI regions were interconnected by the insulation of the PMMA regions. With the addition of PMMA, an increase in conductivity occurred because of electronic tunneling through the nonconducting PMMA separating the mesoscopic conducting PANI islands.

TGA

TGA measurement of nano-PANI was performed under an N_2 atmosphere. The TGA curves for the PANI synthesized in aqueous solution with and without the SDS, NPE, and CTAB micelle templates are compared in Figure 6.

The weight losses observed in the temperature range from room temperature up to 100°C for all of the samples corresponded to water molecules/moisture; this was due to the hygroscopic nature of the polymer. The weight loss of PANI (Fig. 6) at temperatures up to 250°C was attributed to the loss of oligomers, and the weight loss beyond 250°C up to 570°C was due to the degradation and decomposition of the backbone units of PANI. As shown by TGA [Fig. 6(a–d)], the rate of weight loss of PANI was in the following order: PANI–CTAB > PANI–NPE > PANI–SDS > PANI–bulk, respectively.

Although the rates of weight loss of the PANI–PMMA nanocomposites (Fig. 7, curves Ba, Bb, Bc, and Bd) were much slower than that of the corresponding pristine PANI, the results reveal that the inlaid PMMA nanocomposite retarded the thermal decomposition of the polymer chain of PANI in the entire temperature range (100–570°C).

CONCLUSIONS

In this study, anionic (SDS), nonionic (NPE), and cationic (CTAB) micelles were used as polymerization media to produce PANI nanoparticles. The use of surfactants as templates in the synthesis of conducting PANI may offer new possibilities for the fabrication of PANIs with different morphologies, thermal stabilities, and conductivities. PANI–PMMA nanostructure composites were synthesized *in situ*. We found that the nanocomposites had a good thermal stability and higher electrical conductivity than the pristine polymer.

References

1. Unsworth, J.; Lunn, B. A.; Innis, P. C.; Jin, Z.; Kaynak, A.; Booth, N. G. J Intell Mater Syst Str 1992, 3, 380.
2. Schoch, K. F., Jr. IEEE Electric Insulat Mag 1994, 10, 29.
3. Angelopoulos, M. IBM J Res Dev 2001, 45, 57.
4. Gospodinova, N.; Terlemezyan, L. Prog Polym Sci 1998, 23, 1443.
5. Kewm, J.; Ha, C. S.; Kim, Y. Macromol Res 2006, 14, 401.
6. Pei, Q.; Yu, G.; Zhang, C.; Yang, Y.; Heeger, A. J. Science 1995, 269, 1086.
7. Asawapirom, U.; Bulut, F.; Farrell, T.; Gadermaier, C.; Gamerith, S.; Guntner, R.; Kietzke, T.; Patil, S.; Piok, T.; Montenegro, R.; Stiller, B.; Tiersch, B.; Landester, K.; List, E. J. W.; Neher, D.; Torres, C. S.; Scherf, U. Macromol Symp 2004, 212, 83.
8. Chaudhuri, D.; Kumar, A.; Rudra, I.; Sarma, D. D. Adv Mater 2001, 13, 1548.
9. Zhang, X.; Gous, W. J.; Manohar, S. K. J Am Chem Soc 2004, 126, 4502.
10. DePaoli, M. A. In Handbook of Organic Conductive Molecules and Polymers; Nalawa, H. S., Ed; Wiley: New York, 1997; Vol. 2.
11. Omastova, M.; Pionteck, J.; Kosina, S. In Electronic and Optical Properties of Conjugated Molecular Systems in Condensed Phases; Hotta, S., Ed.; Research Signpost: Kerala, India, 2003; p 153.
12. Bhadra, S.; Khastgir, D. Eur Polym J 2007, 43, 4332.
13. Bhadra, S.; Singha, N. K.; Khastgir, D. J Appl Polym Sci 2008, 107, 2486.
14. Bhadra, S.; Singha, N. K.; Khastgir, D. Curr Appl Phys 2009, 9, 396.
15. Bhadra, S.; Singha, N. K.; Khastgir, D. Polym Eng Sci 2008, 48, 995.
16. Sinha, S.; Bhadra, S.; Khastgir, D. J Appl Polym Sci 2009, 112, 3135.
17. Bhadra, S.; Khastgir, D. J Appl Polym Sci 2009, 114, 238.
18. Cho, M. S.; Park, S. Y.; Hwng, J. Y.; Choi, H. J. Mater Sci Eng C 2004, 24, 15.
19. Rao, P. S.; Subrahmanya, S.; Sathyanarayana, D. N. Synth Met 2003, 139, 397.
20. Barra, G. M. O.; Leyva, M. A.; Soares, B. G.; Mattoso, L. H.; Sens, M. J Appl Polym Sci 2001, 82, 114.

21. Aksimentyeva, O.; Konopetnyk, O.; Opaynych, I.; Tsizh, B.; Ukrainets, A.; Ulansky, Y.; Martyniuk, G. Rev Adv Mater Sci 2010, 23, 185.
22. Sivakkumar, S. R.; Kima, W. J.; Chou, J. A.; MacFariane, D. R.; Forsyth, M.; Kima, D. W. J Power Sources 2007, 171, 1062.
23. Erokhin, V.; Berzina, T.; Fontana, M. P. J Appl Phys 2005, 97, 064501.
24. Ramya, G.; Renugadevi, C.; Rao, C. R. K.; Trivedi, D. C. React Funct Polym 2008, 68, 701.
25. Chiou, N. R.; Epstein, A. J. Adv Mater 2005, 17, 1679.
26. Steijskal, J.; Sapurina, I.; Trchova, M.; Konyushenko, E. N.; Holler, P. Polymer 2006, 47, 8253.
27. Jang, J.; Ha, J.; Kim, S. Macromolecular Res 2007, 15, 154.
28. Fendler, J. H. Membrane Mimetic Chemistry: Characterizations and Applications of Micelles, Microemulsions, Monolayers, Bilayers, Vesicles, Host–Guest Systems, and Polyions; Wiley: New York, 1982; pp 6, 206.
29. Liu, W.; Cholli, A. L.; Nagarajan, R.; Kumar, J.; Tripathy, S. K.; Senecal, K. J.; Bruno, F. B.; Samuelson, L. A. J Am Chem Soc 1999, 121, 11345
30. Liu, W.; Kumar, J.; Tripathy, S. Langmuir 2002, 18, 9696.
31. Missel, P. J.; Mazer, N. A.; Carey, M. C.; Benedek, G. B. J Phys Chem 1989, 93, 8354.
32. Kim, B.-J.; Oh, S.-G.; Han, M.-G.; Im, S.-S. Langmuir 2000, 16, 5841.
33. Rosen, M. J. Surfactants and Interfacial Phenomena, 2nd ed.; Wiley: New York, 1989.
34. Yan, F.; Xue, G. J Mater Chem 1999, 9, 3035.
35. Pillai, V.; Kumar, P.; Hou, M. J.; Ayyub, P.; Shah, D. O. Adv Colloid Interface Sci 1995, 55, 241.
36. Amrithesh, M.; Aravind, S.; Jayalekshmi, S.; Jayasree, R. S. J Alloys Compd 2008, 449, 176.